buildings

MDPI

Article

Human-Induced-Vibration Response Analysis and Comfort Evaluation Method of Large-Span Steel Vierendeel Sandwich Plate

Lan Jiang [1,2], Ruoheng Cheng [1,2], Huagang Zhang [3,*] and Kejian Ma [3]

[1] Hubei Provincial Engineering Technology Research Center for Power Transmission Line, China Three Gorges University, Yichang 443002, China
[2] College of Electrical Engineering & New Energy, China Three Gorges University, Yichang 443002, China
[3] Space Structures Research Center, Guizhou University, Guiyang 550025, China
* Correspondence: hgzhang@gzu.edu.cn

Abstract: A steel Vierendeel sandwich plate used as a large-span lightweight floor structure for vibration comfort during crowd gatherings was considered. Taking the steel Vierendeel sandwich plate in Guizhou Museum as an example, through finite element transient analysis, the effects of the structural damping, pedestrian self-weight, floor span, surface concrete slab thickness, and structural parameters on the floor's acceleration response distribution were deeply studied. According to the distribution characteristics of the acceleration response, a distribution model function was constructed, and a distribution Gauss model of the relationship between the peak acceleration response and the position of the steel Vierendeel sandwich plate was established. A field test of the sandwich plate under human-induced fixed-point excitation was carried out, and the model fitting results were compared with the actual test results. The results showed that the Gaussian model could effectively estimate the peak acceleration response at different positions on the floor. In addition, according to the distribution model, a comfort evaluation method based on the comfort assurance rate was proposed that could greatly reduce the representative value of the acceleration evaluation. The research results provide a reference for the comfort evaluation and corresponding vibration-reduction design of long-span steel Vierendeel sandwich plates.

Keywords: Vierendeel sandwich plate; comfort evaluation; human-induced load; acceleration response distribution

Citation: Jiang, L.; Cheng, R.; Zhang, H.; Ma, K. Human-Induced-Vibration Response Analysis and Comfort Evaluation Method of Large-Span Steel Vierendeel Sandwich Plate. *Buildings* **2022**, *12*, 1228. https://doi.org/10.3390/buildings12081228

Academic Editors: Jun Chen and Haoqi Wang

Received: 20 June 2022
Accepted: 9 August 2022
Published: 12 August 2022

1. Introduction

With the progress of building technology and the application of high-strength materials, "Large span, low self weight and low damping" is the development direction of building structures, and various types of long-span floor forms have been invented [1,2]. The Vierendeel sandwich plate is a new type of structure that is widely used in long-span industrial and public buildings. Crowd aggregation is inevitable during normal use of floors. A floor is characterized by light weight and small vertical stiffness. A large vibration response is easily produced under a pedestrian load. At the least, it will cause people's discomfort, and at the worst, it will lead to fatigue damage of the floor and reduce the service life of the structure [3,4]. Historically, the Millennium Bridge in London, Techno Mart building in Korea, and other projects had to be stopped due to excessive human-induced-vibration response. It can be seen that the structural vibration caused by a human-induced load has become a problem that must be considered in the design of long-span structures.

A hollow sandwich plate is a bidirectional stress hollow structure that is composed of a surface concrete slab, top and bottom chords, and shear connectors. Compared with the general frame structure, bidirectional stress, good integrity, and the use of less steel are its characteristics. The structure of a Vierendeel sandwich plate is shown in Figure 1.

It has a wide application prospect in large-span multistory buildings [5]. As a large-span, lightweight floor structure, a steel Vierendeel sandwich plate may be sensitive to vibration due to its own structural characteristics. It is necessary to deeply study the influence of human-induced loads on Vierendeel sandwich plates, as well as the comfort evaluation method.

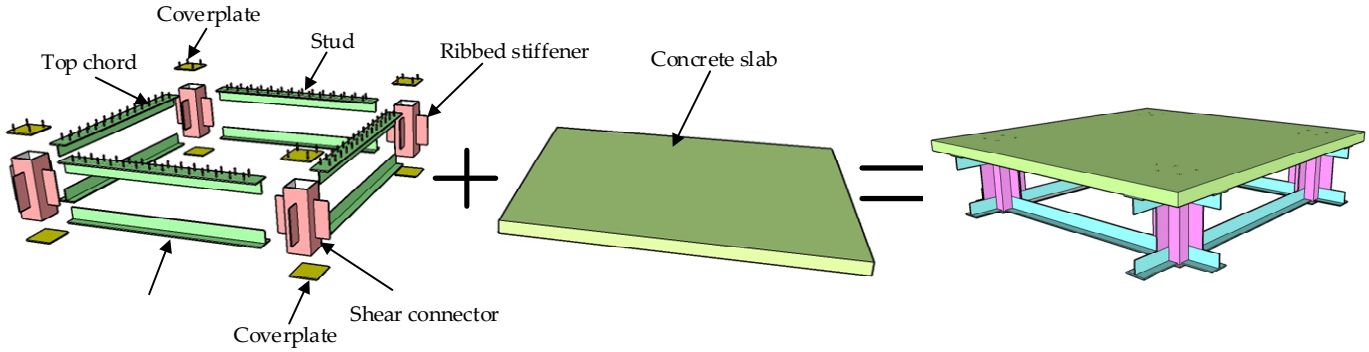

Figure 1. Physical model diagram of Vierendeel sandwich plate.

At present, the human-induced-load model and comfort evaluation standards are the main research directions of domestic and foreign scholars on the human-induced vibration of long-span floors. For the study of loads, the load model is mainly established on the basis of the single-step drop test. Based on a large number of tests, a variety of periodic walking load models have been proposed by researchers [6–8]. On this basis, Chen Jun et al. used the probability density evolution method to analyze the impact of load randomness on the vibration response of a floor. It was considered that the randomness of the pedestrian load had a significant influence on the vibration response of the floor, and the randomness of the pedestrian load should be considered in the comfort evaluation of the floor [9]. In terms of comfort assessment, the current project was mainly implemented with reference to some national or industrial standards. Standards set by the American Institute of Steel Construction [10] and Precast/Prestressed Concrete Institute [11], as well as in the UK Concrete Society's *Technical Report No. 43* [12] and the Concrete Centre's *CCP-016* [13] are widely used. Human-induced loads are divided into general walking loads and rhythmic loads under AISC and PCI standards, and different acceleration limits and frequency limits are given. *CCP-016* states that when the first natural vibration frequency of a floor is lower than 4.2 times the fundamental frequency of the pedestrian load, resonance will occur; and when the first natural frequency of the floor is greater than 4.2 times the fundamental frequency of the pedestrian load, the floor vibration is mainly caused by effective impact. Two methods that can be used to evaluate the structural comfort are proposed in the UK standards. One is the evaluation method based on the response factor, which assumes that the floor vibration is continuous and of the same amplitude. Another evaluation method is based on the vibration dose value, which considers a possible pause in the vibration process and the impact of different vibration amplitudes on human comfort, and can be used for long-term evaluation of the comfort degree. In a comfort evaluation, the analytical or numerical calculation results are usually directly compared with the standard values used in the engineering community to determine the comfort level. However, the span of a long-span floor can reach tens of meters, and pedestrian comfort is affected by the spatial and temporal distribution characteristics of the stimulated points and the feeling points. Therefore, it is of great significance to study the human-induced-vibration response distribution of long-span floors for reasonable evaluation of comfort performance.

Many scholars have studied the vibration comfort of structures. The most basic research on comfort is the human motivation model. The human-induced motivation mode is the most basic research of comfort. In 1961, Harper completed the earliest walking load test with a force-measuring plate, and stated that the walking load curve was M-shaped [6]. Subsequently, several researchers tested the load of human walking using the

direct or indirect method [7,14] and analyzed the influence of walking speed, shoe type, ground characteristics, and other factors on the load model. Chen et al. adopted optical motion-capture technology in which the reflective marks of key parts of the human body were captured by high-speed infrared cameras [15]. This was used to identify the human motion space trajectory to obtain human walking parameters. At present, the time-domain model of load is mainly used in the comfort analysis of structures. The Fourier series model was the most commonly used in existing pedestrian load model research. The dynamic load factor is included in the Fourier series model, and the load mode is directly affected by the value of the dynamic load factor. Therefore, the dynamic load factor has been studied by many researchers [8,16]. In conclusion, it is generally believed that the vertical first-order dynamic load factor is around 0.3~0.5. In terms of the comfort analysis method, the time-domain analysis method based on finite elements is an effective method. Zhu et al. considered the interaction between pedestrians and structures, and used an ANSYS finite element software simulation to study the structural vibration comfort of a two-story cantilevered steel truss floor deck in the Gansu Science and Technology Museum as the engineering background [17]. Cao et al. conducted an experimental study of the human-induced vibration of a large-span composite floor based on a single-person foot-load model in order to meet the comfort requirements and control the floor [18]. Wang et al. carried out an human-induced-vibration test and an ANSYS finite element analysis of a large-scale glulam arch bridge model in order to study the human-induced-vibration characteristics of a wooden-structure pedestrian bridge [19]. Peak acceleration is used for comfort performance evaluation. Based on the walking route method, the vibration comfort performance of a steel Vierendeel sandwich plate was analyzed by Jiang et al. under different walking routes [20]. Based on the existing load model, a finite element numerical calculation method was adopted in the above research to analyze the maximum response of different types of structures under human-induced excitation and to evaluate the comfort. However, for long-span floors, the vibration responses of different positions on the floor will differ greatly under human-induced excitation. If the maximum response is simply used to evaluate the comfort of the entire floor, the evaluation will inevitably be too conservative. Therefore, for large-span floor structures such as a Vierendeel sandwich plate, it is necessary to analyze the vibration-response-distribution characteristics of the floor under human-induced excitation in order to provide a basis for the reasonable evaluation of comfort performance.

For the evaluation of comfort, there are mainly two methods: one is to limit the natural vertical vibration frequency of the floor above a certain value, which is called the frequency threshold method. Another method requires that the dynamic response (such as acceleration and speed) of the floor under a given human-induced load does not exceed a certain limit, which is called the dynamic response threshold method. The dynamic response threshold method is widely used because it considers multiple factors of floor vibration and can better evaluate comfort. In the evaluation, the vibration acceleration response is often used as the index. Under the British BS 5400 standard [21], the peak acceleration of the structure is used as the pedestrian comfort limit index, and a function of the vertical first-order frequency of the floor is given as the acceleration limit. Similar acceleration limits are also given in the European EN 1990 standard [22]. The International Organization for Standardization stipulates in its ISO 10137 that when the acceleration response is less than the vibration comfort limit, the comfort is considered to meet the requirements; otherwise, the comfort is considered to not meet the requirements [23]. The German EN03 standard states that pedestrian comfort cannot be simply divided into comfort and discomfort. The vibration comfort level should be divided in detail according to the natural vibration frequency and structural acceleration response [24]. The Chinese specifications GB50010-2010 [25] and JGJ3-2010 [26] refer to ISO standards, and the peak acceleration limits for floors with different natural frequencies are given. Among the above standards, the evaluation of peak acceleration is adopted in BS 5400, EN 1990, EN03, and Chinese standards, and the evaluation of peak acceleration and RMS acceleration is

adopted in ISO 10137. In the application of standards, Fiore et al. proposed a practical probabilistic method for evaluating bridge reliability based on a histogram. Useful estimates of the probability of exceeding the predefined human sensitivity limit were provided by histograms [27]. The above published standards provides references for the evaluation of the human-induced-vibration comfort of large-span Vierendeel sandwich plates.

In this paper, the steel Vierendeel sandwich plate at the Guizhou Museum was taken as the research object. According to the functional characteristics of steel Vierendeel sandwich plates, the response characteristics of the floor with time and space were analyzed using a time-domain method, and the effects of different factors on the acceleration-response distribution were studied. A corresponding distribution mathematical model was constructed, and a comfort evaluation method based on the floor area comfort assurance rate was proposed.

2. Distribution Rule of Vibration Response of Vierendeel Sandwich Plates

2.1. Finite Element Model

Orthogonally placed Vierendeel sandwich plates are widely used in engineering, and are the most representative. A steel Vierendeel sandwich plate was used as the analysis object in this study. A steel Vierendeel sandwich plate is a two-way stress structure, and its plane aspect ratio is generally close to one. The size parameters of the structure are shown in Table 1, and schematic diagram showing the size of each component of the structure is presented in Figure 2. In order to analyze the vibration response characteristics of a steel Vierendeel sandwich plate under human-induced excitation, a typical size floor slab was designed, and the basic size of the structure is shown in Table 2. The surface concrete slab structure adopted C30 grade concrete, and the steel structures such as the top and bottom chords and the shear connectors adopted Q345B steel. The material parameters are shown in Table 3. Jiang et al. showed that the dynamic characteristics of a solid–shell model of a steel Vierendeel sandwich plate were closest to the actual structure [28]. Therefore, a solid–shell finite element model of the steel Vierendeel sandwich plate was established in ANSYS software, as shown in Figure 3. Since the top (bottom) chords, shear connectors, and ribbed stiffener of the T-section steel were all thin-walled structures, four-node spatial elastic shell elements were used. The thickness of surface concrete slab was larger than the span of the slab, so eight-node 3D solid elements were used. In practical engineering, a surface concrete slab is reliably connected to the top chords through studs. In the finite element model, the top chords and concrete slab adopted a shell element and a solid element, respectively, and the numbers of node degrees of freedom of these two element types were different. Therefore, the degrees of freedom of the top chords' flange and the concrete slab's nodes at the corresponding positions were coupled to realize the deformation coordination between different elements. Steel Vierendeel sandwich plates are generally rigidly connected to steel columns at the surrounding nodes. Ref. [28] discussed the influence of three different boundary conditions on the dynamic characteristics of the floor. The results showed that the dynamic characteristics of the floor were closer to the measured values when fixed constraints were applied to the intersection of the grid. In summary, in the numerical calculation, the translational and rotational degrees of freedom of the grid intersections around the floor were constrained (Figure 2a).

Table 1. Structural size parameter symbols.

Parameter Name	Symbol	Parameter Name	Symbol
Floor span	L	Grid size	a
Grid number	n	Total height (excluding concrete slab)	h
Chord height	h_1	Chord width	b_1
Chord flange thickness	t_f	Chord web thickness	t_w
Shear connector thickness	t_p	Ribbed stiffener width	b_t
Concrete slab thickness	δ	Shear connector width	b_2
Ribbed stiffener thickness	t_t	-	-

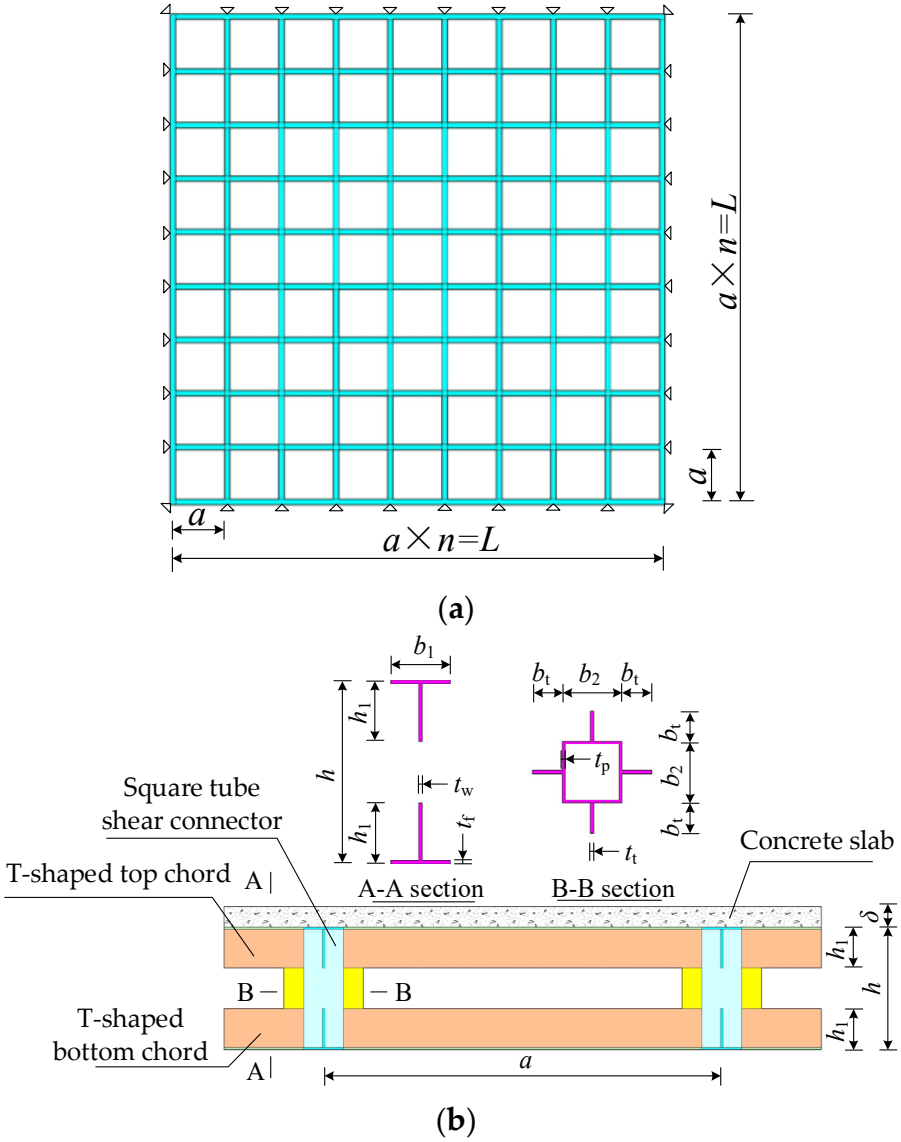

Figure 2. Structural size diagram: (**a**) plane layout; (**b**) structural details.

Table 2. Basic parameters of model structure.

Span/L (m)	Grid Size/a (m)	Overall Height/h (mm)	Chord Height/h_1 (mm)	Chord Width/b_1 (mm)
18	2	600	200	200
Chord flange thickness/t_f(mm)	Ribbed stiffener width/b_t (mm)	Shear connector thickness/t_p (mm)	Ribbed stiffener thickness/t_t (mm)	Concrete slab thickness/δ (mm)
8	100	6	8	100

Table 3. Material physical parameters.

Material	Modulus of Elasticity (MPa)	Poisson's Ratio	Density (kg/m^3)
Q345 steel	2.06×10^5	0.3	7850
C30 concrete	3.00×10^4	0.2	2500

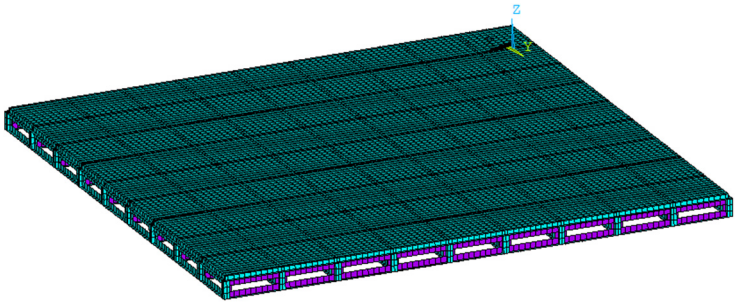

Figure 3. Finite element model of Vierendeel sandwich plate.

The human-induced excitation load was applied in the finite element model of the floor, and a finite element transient dynamic response analysis was carried out to acquire the distribution rule of the acceleration response. The step-by-step integration method was used in the analysis, and the Rayleigh damping model was used; the damping ratio reference value was 0.02. While considering that a multi-person excitation condition is generally expressed as the product of the calculation results of the single-person excitation condition and the effect coefficient, we analyzed the corresponding characteristics of the floor under fixed-point excitation; that is, under the condition of marching on the spot by a single person. The load model adopted the walking excitation parameter model recommended by the International Association for Bridge and Structural Engineering (IABSE), as shown in Equation (1):

$$F_P(t) = G[1 + \sum_{i=1}^{3} \alpha_i \sin(2i\pi f_s t - \Phi_i)] \quad (1)$$

where F_P is the exciting force, G is the weight of human beings, i is the ith order, α_i is the dynamic load factor of the ith order load frequency, f_s is the walk frequency, and Φ_i is the phase angle of the ith order load frequency. The dynamic load factor has been studied by many researchers; Blanchard proposed a first-order sine harmonic model with a dynamic load factor of 0.257 [29]. Based on three-dimensional motion capture technology and a large amount of data, Chen Jun gave the value of the dynamic load factor: $\alpha_1 = 0.235f_s - 0.2010$, $\alpha_2 = 0.0949$, $\alpha_3 = 0.0523$, which was in line with the body characteristics of Chinese people [8], so this value was used as the calculation condition of this paper.

Matsumoto analyzed the probability distribution characteristics of walking frequency through a random sampling test and found that human walking frequency obeyed the normal distribution, with a mean value of 2.0 Hz and a standard deviation of 0.173 Hz [30]. Han X believed that human self-weight obeyed a normal distribution, with a mean of 700 N and a standard deviation of 145 N [31]. The value range of load parameters is shown in Table 4. Therefore, in the analysis of human-induced-vibration response characteristics, the walking frequency was 2 Hz and the weight of the human was 700 N.

Table 4. Value range of load parameters.

Parameter	Mean Value	Variation Range
Walking frequency/Hz	2.0	1.6/1.8/2.0/2.2/2.4
Human weight/N	700	555/600/650/700/750/800/845

2.2. Response Characteristics of Human-Induced Vibration

To perform a transient analysis of the acceleration response of the floor, the position of both the pedestrian load and the structural vibration response receiver should be determined first. There are two main principles for selecting loading points: one is whether the response generated by the excitation at this point is the most unfavorable, and the other is whether the excitation at this point occurs easily under actual working conditions. The location of the vibration receiver also follows two principles: whether the position of the

receiver is the most unfavorable, and where it is prone to occur. In view of this, two issues were mainly analyzed in this paper: the effect of different point of excitations on the peak response and the acceleration response distribution at different positions under the same point of excitation.

2.2.1. Effect of Substructure on Floor Acceleration

As a special form of floor structure, a Vierendeel sandwich plate has great differences in the section size at each point of the plane. Figure 4 shows a grid diagram of the Vierendeel sandwich plate. In the figure, the points of shear connectors on the slab are shown by D, F, G and I; the points of the top chords on the Vierendeel beam are shown by B, C, E and H; and A is the point at the center of the plane of the concrete slab.

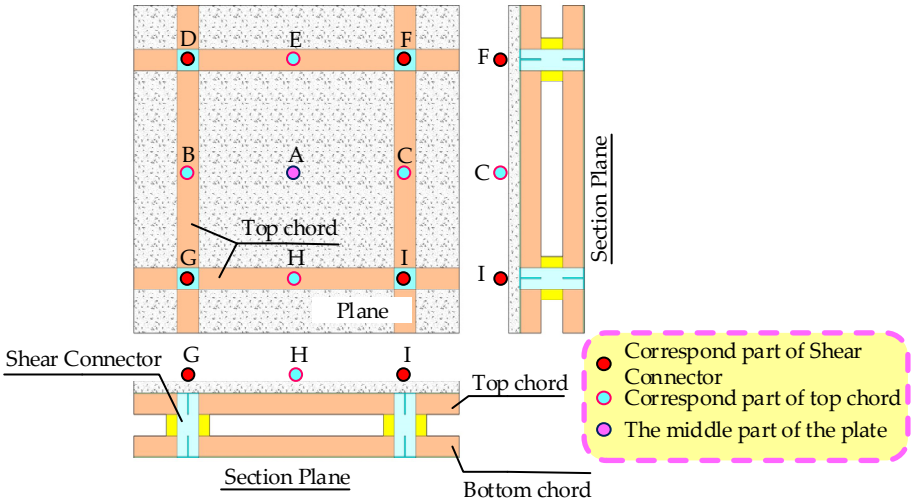

Figure 4. Schematic diagram of typical parts of floor.

In order to analyze whether the acceleration response at different positions on the floor was affected by the characteristics of the substructure, the peak acceleration responses at the different positions shown in Figure 4 were compared, as shown in Figure 5. It can be seen in Figure 5 that under the conditions of different concrete slab thicknesses, an approximately linear distribution was displayed by the DEF and BAC values. This showed that the peak acceleration response on the Vierendeel sandwich plate was hardly affected by the different positions, and the effect of this factor could be ignored when selecting the sensing point.

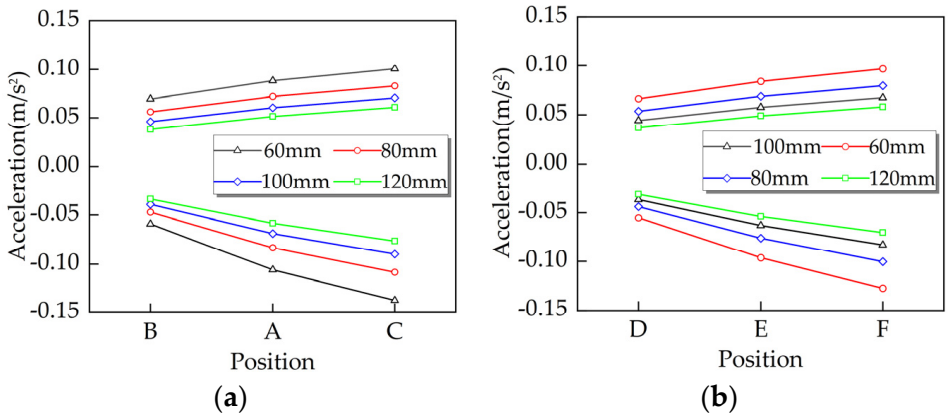

Figure 5. The effect of different positions on the plane on the peak acceleration: (**a**) point DEF; (**b**) point BAC.

2.2.2. Effect of Point of Excitation Position on Floor Acceleration

To study the effect of the point-of-excitation position on the peak dynamic response of the floor, nine typical points of excitation (points A~I) were determined on the floor; these positions are shown in Figure 6.

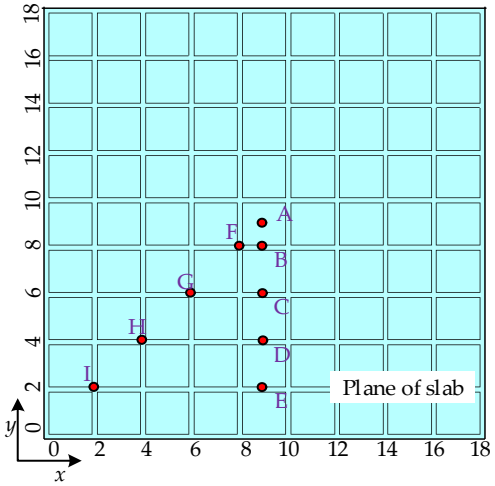

Figure 6. Distribution diagram of points of excitation.

The peak acceleration distribution of each part of the floor under fixed-point excitation when the point of excitation was located at the geometric center of the floor (point A) is shown in Figure 7. It can be seen in the figure that the acceleration response was funnel-shaped on the floor: the closer to the point of excitation, the greater the absolute value of the peak acceleration.

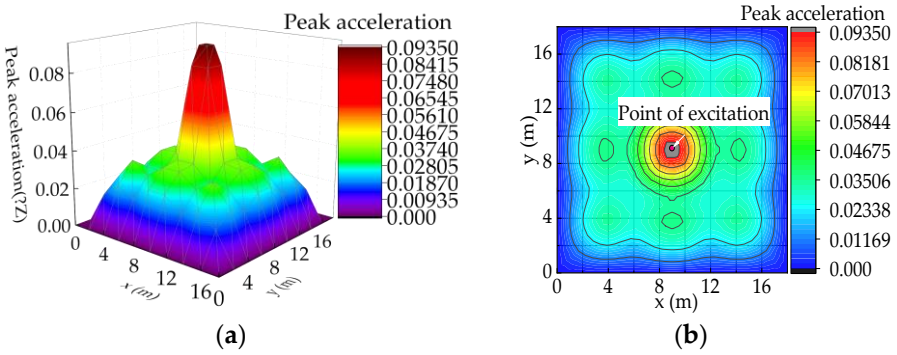

(**a**) (**b**)

Figure 7. Acceleration distribution of point A: (**a**) peak acceleration diagram; (**b**) peak acceleration contour map.

When the point of excitation was located on the nongeometric center of the floor (points B~I), the dynamic response of the floor was calculated and the acceleration peaks at different positions of the floor were extracted; the contour map was drawn as shown in Figure 8. As can be seen in Figure 8, in general, the closer to the point of excitation, the greater the floor's response peak, and its maximum value is located at the point of excitation. In addition, the closer to the point of excitation, the denser the contour line. The acceleration peak on the floor decreased exponentially with the increase in the distance between the sensing point and the point of excitation. It should be noted that when the point of excitation was close to the constrained edge of the floor (points E and I), the acceleration peak of floor was no longer at the point of excitation, but was near the point of excitation.

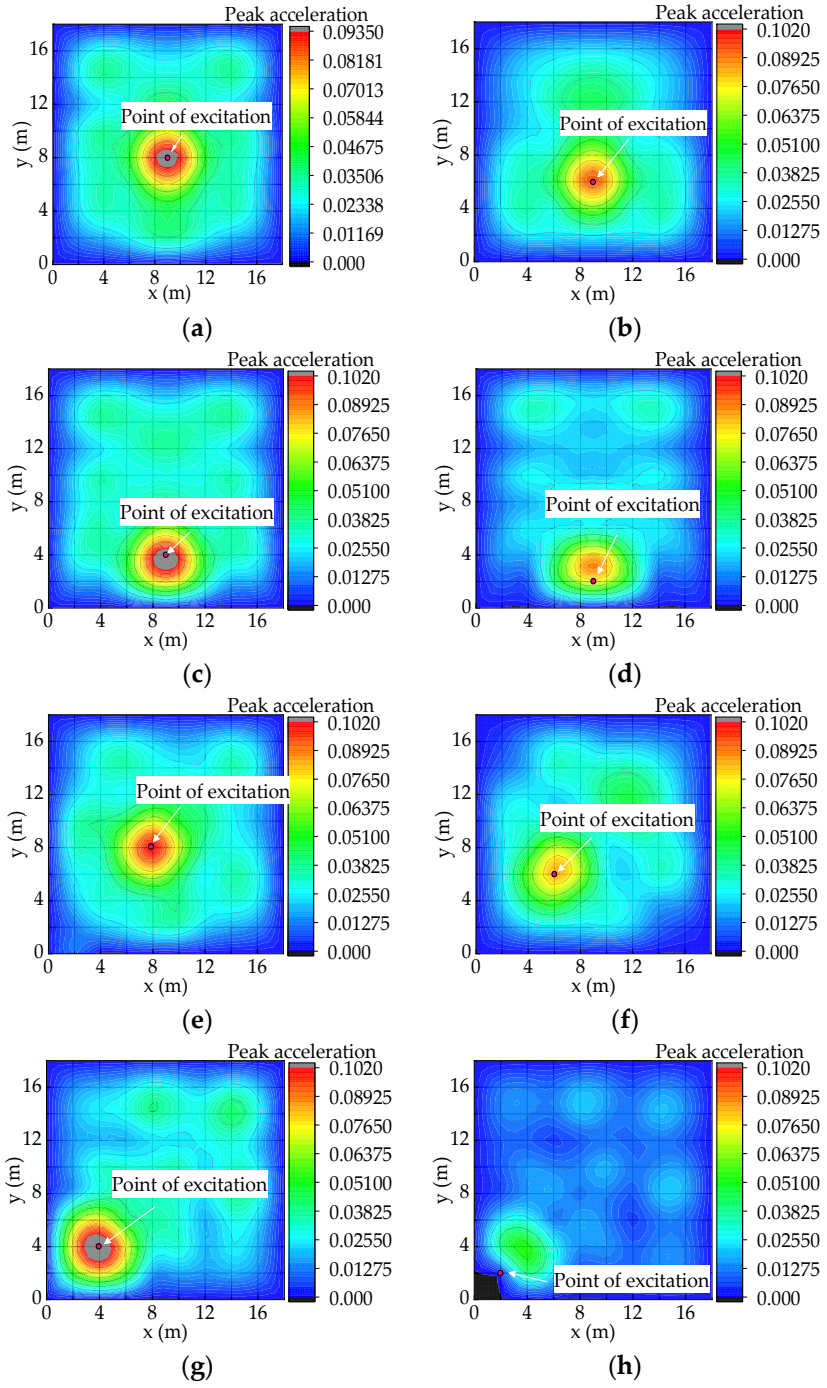

Figure 8. Contour map of peak acceleration: (**a**) point B; (**b**) point C; (**c**) point D; (**d**) point E; (**e**) point F; (**f**) point G; (**g**) point H; (**h**) point I.

2.2.3. Effect of Damping on Floor Acceleration

The amount of mechanical energy loss in a floor system is described as damping, and is usually expressed as the ratio of actual damping to critical damping; that is, the damping ratio. During the calculation, the first two natural frequencies and corresponding damping ratios were directly defined, then the damping in the model was calibrated using mass and stiffness matrix modifiers, which can be obtained using Equations (2) and (3):

$$\alpha = \frac{2\omega_1\omega_2(\omega_1\xi_2 - \omega_2\xi_1)}{{\omega_1}^2 - {\omega_2}^2} \quad (2)$$

$$\beta = \frac{2(\omega_1 \xi_1 - \omega_2 \xi_2)}{{\omega_1}^2 - {\omega_2}^2} \tag{3}$$

where α and β are the mass and stiffness matrix modifiers, respectively; ω_i is the natural frequency of the ith order; and ξ_i is the damping ratio of the ith mode (i = 1, 2).

The damping matrix [C] is a linear combination of the mass matrix [M] and the stiffness matrix [K]. This damping, which is called Rayleigh damping, can be calculated using Equation (4):

$$[C] = \alpha[M] + \beta[K] \tag{4}$$

Floor damping includes floor damping and nonstructural damping. Structural materials, the floor system, the building structure, and other factors will affect the damping; as affected by various factors, floor damping is generally between 2% and 10%. The effect of damping change on the acceleration response of a floor slab under a human-induced load is discussed in this paper. We took the point of excitation at the geometric center as an example, and assumed that the coordinate origin coincided with the geometric center of the floor. The peak acceleration response distribution of the hollow steel sandwich plate when the floor damping was varied between 2% and 8% is shown in Figure 9.

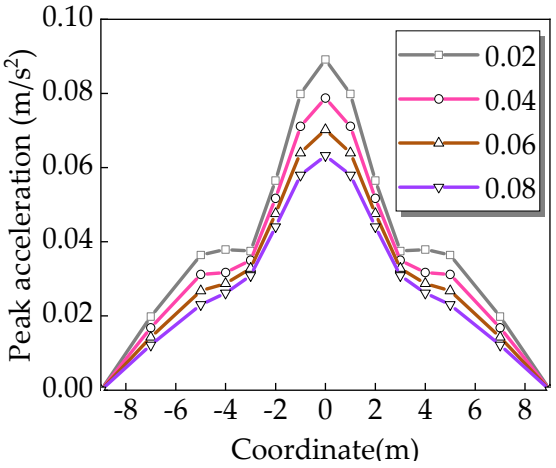

Figure 9. Effect of damping on peak acceleration response.

It can be seen in the above figure that when the damping was increased, the peak acceleration around the floor decreased significantly. This showed that increase in the structural damping had a significant effect on reducing the vibration response of the floor.

2.2.4. Effect of Load Parameters on Floor Acceleration

The main parameters that affect continuous walking excitation are walking frequency, self-weight, and other factors. Experimental research has shown that in general, the frequency of natural human walking is between 1.6 and 2.4 Hz. In order to study the influence of walking frequency on the structural response, this paper constructed pedestrian load curves under different frequencies, as shown in Figure 10, and the acceleration response of the floor under different pedestrian excitation frequencies was respectively calculated. The peak acceleration response distribution at different positions on the floor is shown in Figure 11 (assuming that the coordinate origin coincided with the geometric center of the floor). It can be seen in the figure that the distribution of peak acceleration on the floor was similar under different excitation frequencies. With an increase in the excitation frequency, the peak acceleration of the floor increased gradually.

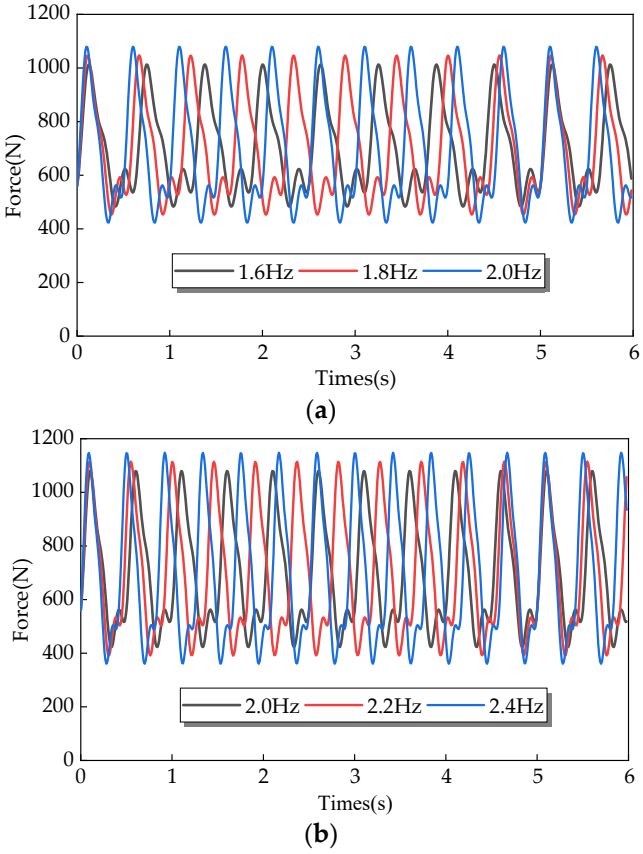

Figure 10. Pedestrian loads with different frequencies: (**a**) walking frequencies of 1.6 Hz, 1.8 Hz, and 2.0 Hz; (**b**) walking frequencies of 2.0 Hz, 2.2 Hz, and 2.4 Hz.

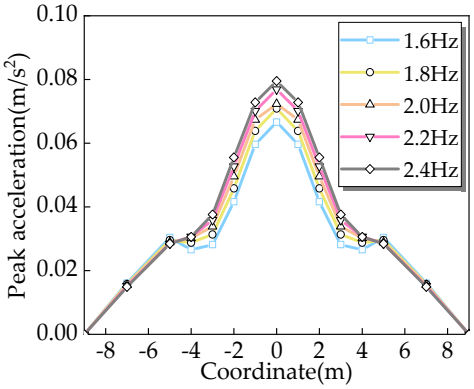

Figure 11. Effect of load frequency on peak acceleration response.

The peak value of the pedestrian load curve and the human-induced-load response of a floor are directly affected by human weight. The general value for a pedestrian load is 700 N according to [32], while the body weight of adults varies in the range of 700 ± 145 N according to [31]. In order to analyze the influence of human body weight on the peak response of the floor, load curves with adult self-weights of 555 N, 600 N, 650 N, 700 N, 750 N, 800 N, and 845 N were constructed (Figure 12), and then we analyzed the acceleration response. The peak acceleration distribution of the floor is shown in Figure 13 (assuming that the coordinate origin coincided with the geometric center of the floor). It can be seen in the figure that self-weight had a significant impact on the peak response of the floor caused by a human-induced load. With the increase in self-weight, the peak value of floor response increased significantly.

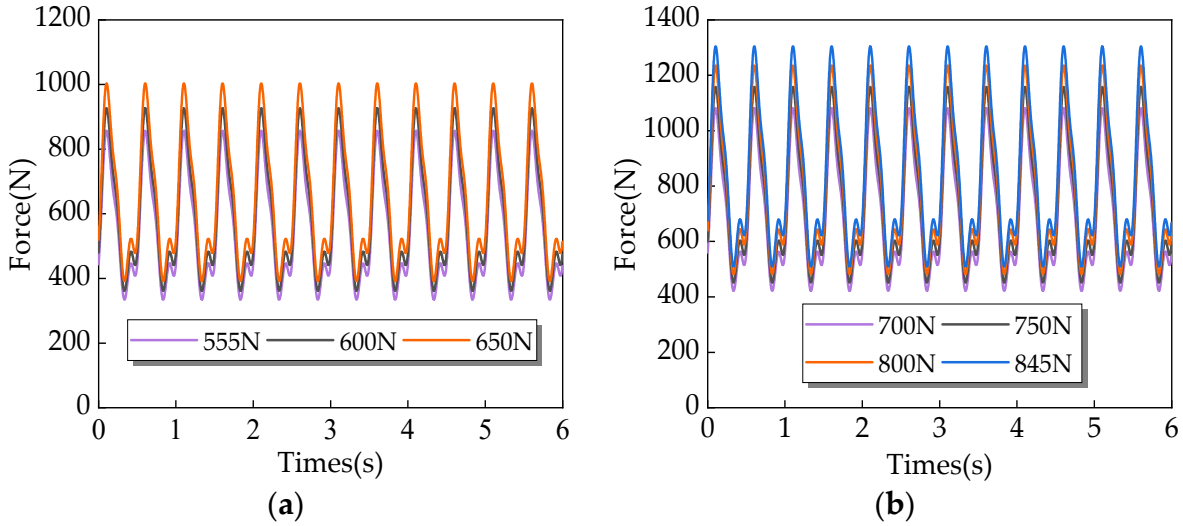

Figure 12. Pedestrian loads with different human weights: (**a**) human weights of 555 N, 600 N, and 650 N; (**b**) human weights of 700 N, 750 N, 800 N, and 845 N.

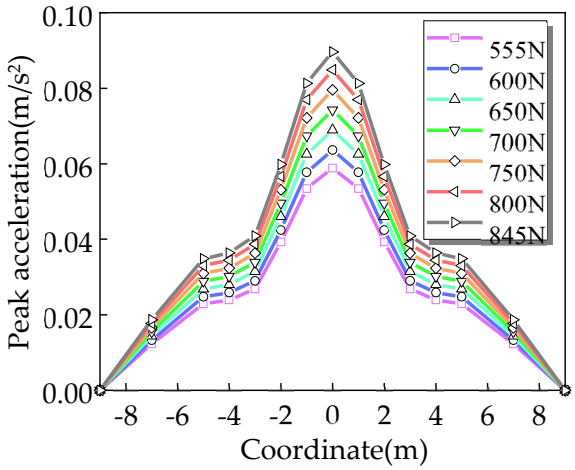

Figure 13. Effect of self-weight on peak acceleration response.

2.2.5. Effect of Structural Parameters on Floor Acceleration

According to [20], the main factors that affect the vertical dynamic characteristics of a Vierendeel sandwich plate are the floor span, grid size, and concrete slab thickness, while the secondary factors are chord height and shear connector thickness. In this paper, these five factors were selected to analyze the effects of structural parameters.

When analyzing the effects of structural parameters, the selected load mode was the same as given above. The human walking frequency was 2 Hz, the human weight was 700 N, and the point of excitation was the geometric center of the floor; that is, point A in Figure 6. When changing the structural parameters, only one variable was changed each time based on the basic model. The basic model parameters were the same as those given in Table 2, and the range of parameter variations is shown in Table 5. Assuming that the coordinate origin coincided with the geometric center of the floor, the damping ratio is 0.05. Through transient dynamic analysis, the peak acceleration profiles at different positions on the floor were obtained, as shown in Figure 14.

Table 5. Variation range of parameters.

Span (m)	Grid Size (mm)	Concrete Slab Thickness (mm)	Chord Height (mm)	Shear Connector Thickness (mm)
14	1500	60	160	5
16	1800	80	180	6
18	2000	100	200	7
20	2250	120	220	8
22	-	140	240	9
24	-	-	-	10

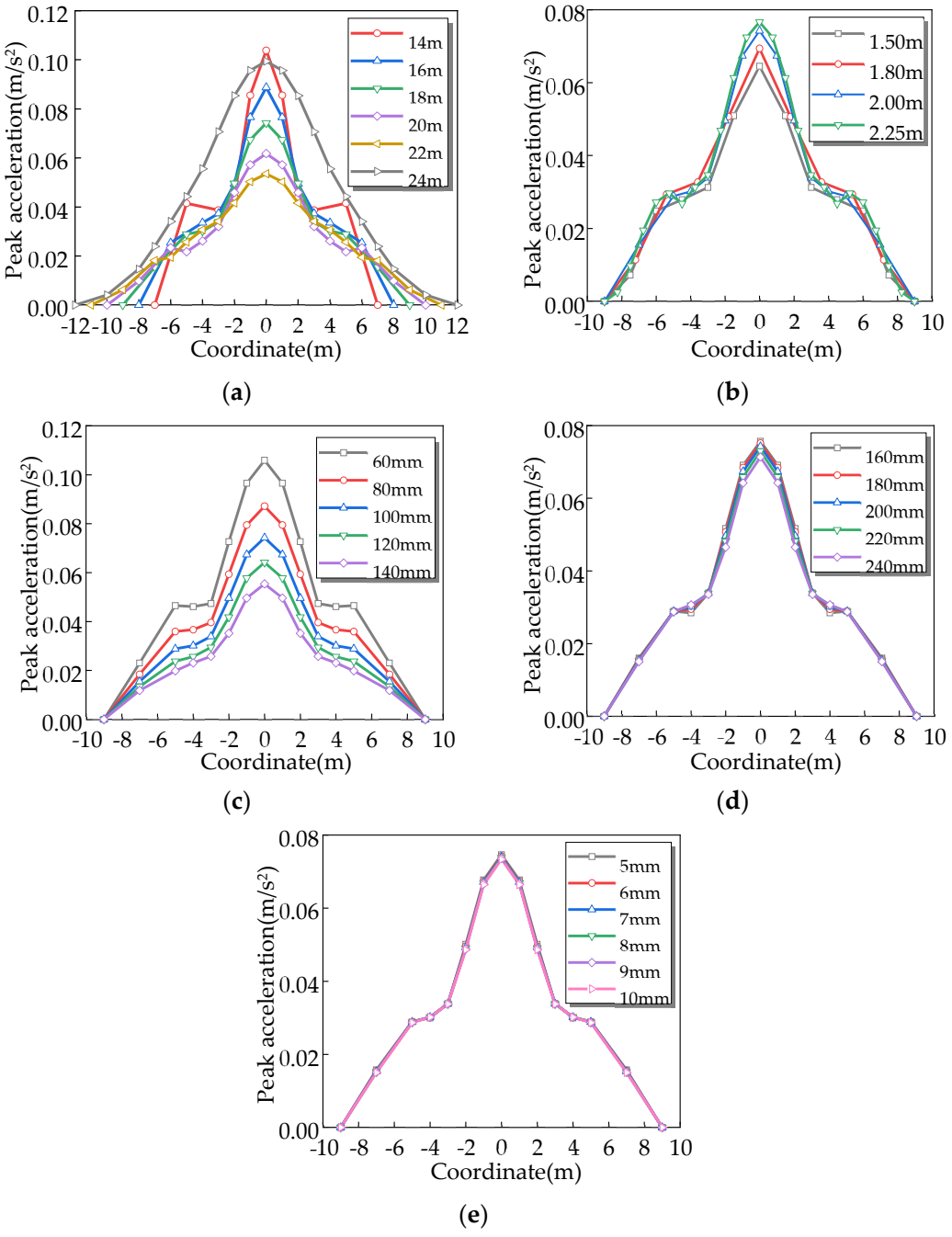

Figure 14. Effect of structural parameters on peak acceleration response: (**a**) effect of floor span; (**b**) effect of grid size; (**c**) effect of concrete slab thickness; (**d**) effect of chord height; (**e**) effect of shear connector thickness.

Figure 14 shows that the human-induced acceleration response was significantly affected by the span of the hollow sandwich plate and the thickness of the concrete plate, and the calculation results were affected by the grid size to some extent. The effects of the chord height and shear connector thickness were very small, so they could not be considered. With the increase of the span of the Vierendeel sandwich plate, the peak acceleration in the center of the span decreased. However, when the span was increased to 24 m (the fundamental frequency was 2 Hz), the peak acceleration response of the floor increased sharply, indicating that the floor resonated with people. With the increase in the thickness of the concrete slab, the peak acceleration response of the floor decreased obviously, and the peak acceleration response decreased with the decrease in the grid size.

3. Construction of Vibration Response Distribution Model

The response characteristics of the steel Vierendeel sandwich plate under human-induced fixed-point excitation were analyzed, and showed that the peak acceleration response of the floor was funnel-shaped in the plane, and the specific distribution shape was related to load parameters, damping, structural parameters, and resonance or lack thereof. In order to establish the distribution model of the acceleration response and position correlation of the Vierendeel sandwich plate under human-induced fixed-point excitation, based on the distribution characteristics of the acceleration response, this paper constructed the distribution model function, and different numerical results were fitted to determine the parameters of the distribution model.

3.1. Gaussian Distribution Model

Floor response can be roughly divided into two categories based on resonance or a lack thereof. When the floor response resonates due to human-induced excitation, the response distribution curve can be expressed by a Gaussian function; and when the curve is symmetrical about the x-axis, it can be expressed using Equation (5)—the curve is shown in Figure 15a. When the floor response does not resonate due to human-induced excitation, the response distribution curve can be expressed by a piecewise function (Equation (6)); the curve is shown in Figure 15b.

$$f(x) = Ae^{-\frac{x^2}{2w^2}} \tag{5}$$

where A is the height of the curve and w is a shape parameter.

$$f(x) = \begin{cases} \frac{2c}{L}x + c & (-\frac{L}{2} \le x < -\frac{L}{3}) \\ \frac{c}{3} + Ae^{-\frac{x^2}{2w^2}} & (-\frac{L}{3} \le x \le \frac{L}{3}) \\ -\frac{2c}{L}x + c & (\frac{L}{3} < x \le \frac{L}{2}) \end{cases} \tag{6}$$

where A is the height of Gaussian distribution curve, c is the parameter, and L is the span of the steel Vierendeel sandwich plate.

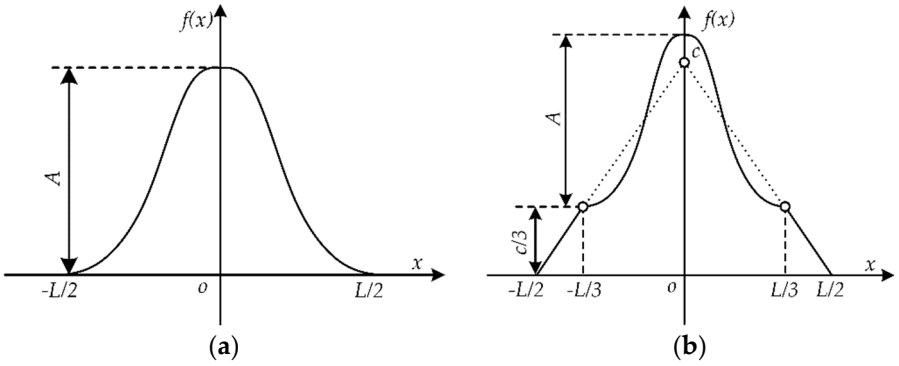

Figure 15. Acceleration response distribution model: (**a**) resonance; (**b**) nonresonance.

The above model is a plane model. For the square plane of the Vierendeel sandwich plate, according to Figure 15b, it can be assumed that the acceleration peak surface was centrosymmetric around the z-axis (x = 0, y = 0). Therefore, the plane Gaussian model could be extended to three-dimensional space, as shown in Equations (7) and (8):

$$f(x,y) = Ae^{-\frac{x^2+y^2}{2w^2}} \tag{7}$$

$$f(x,y) = \begin{cases} \frac{c}{3} + Ae^{-\frac{x^2+y^2}{2w^2}} & (\sqrt{x^2+y^2} \le \frac{L}{3}) \\ -\frac{2c}{L}\sqrt{x^2+y^2} + c & (\frac{L}{3} < \sqrt{x^2+y^2} \le \frac{L}{2}) \end{cases} \tag{8}$$

3.2. Model Parameter Calculation and Quality Evaluation

3.2.1. Parameter Calculation

It can be seen in the above analysis that the peak acceleration distribution was affected by factors, including damping, load frequency, pedestrian self-weight, floor span, grid size, concrete slab thickness, chord height, shear connector thickness, and other structural parameters. Among them, damping, pedestrian self-weight, floor span, and concrete slab thickness were the factors that had a greater influence. In order to simplify the parameter-estimation process, according to [33], the mean value of self-weight was 700 N, the damping ratio was 0.02, the mean value of human walking frequency was 2 Hz, the grid size was 2 m, the chord height was 150 mm, and the shear connector thickness was 5 mm. Different floor span and concrete slab thicknesses were considered, the acceleration response distribution of the square steel Vierendeel sandwich plate was supported by peripheral columns under single-person and fixed-point excitation, and the point of excitation was located in the middle of the span. The specific parameters of the analysis model are shown in Table 6, and the common parameters are shown in Table 7. The analysis model was divided into 2 groups with 5 in each group, for a total of 10.

Table 6. Model parameters.

Specimen	M1 Model					M2 Model				
	M1-1	**M1-2**	**M1-3**	**M1-4**	**M1-5**	**M2-1**	**M2-2**	**M2-3**	**M2-4**	**M2-5**
Span (m)	16	16	16	16	16	24	24	24	24	24
Concrete slab thickness (mm)	60	80	100	120	140	60	80	100	120	140

Table 7. Model common parameters.

Grid Size (mm)	Overall Height (mm)	Chord Height(mm)	Chord Width (mm)
2000	600	150	200
Chord flange thickness(mm)	Chord web thickness (mm)	Shear connector thickness (mm)	Ribbed stiffener thickness (mm)
10	8	5	100

The calculation results of each model were fitted by a nonlinear curve following the formulas of Equations (5) and (6); the fitting curve is shown in Figure 16.

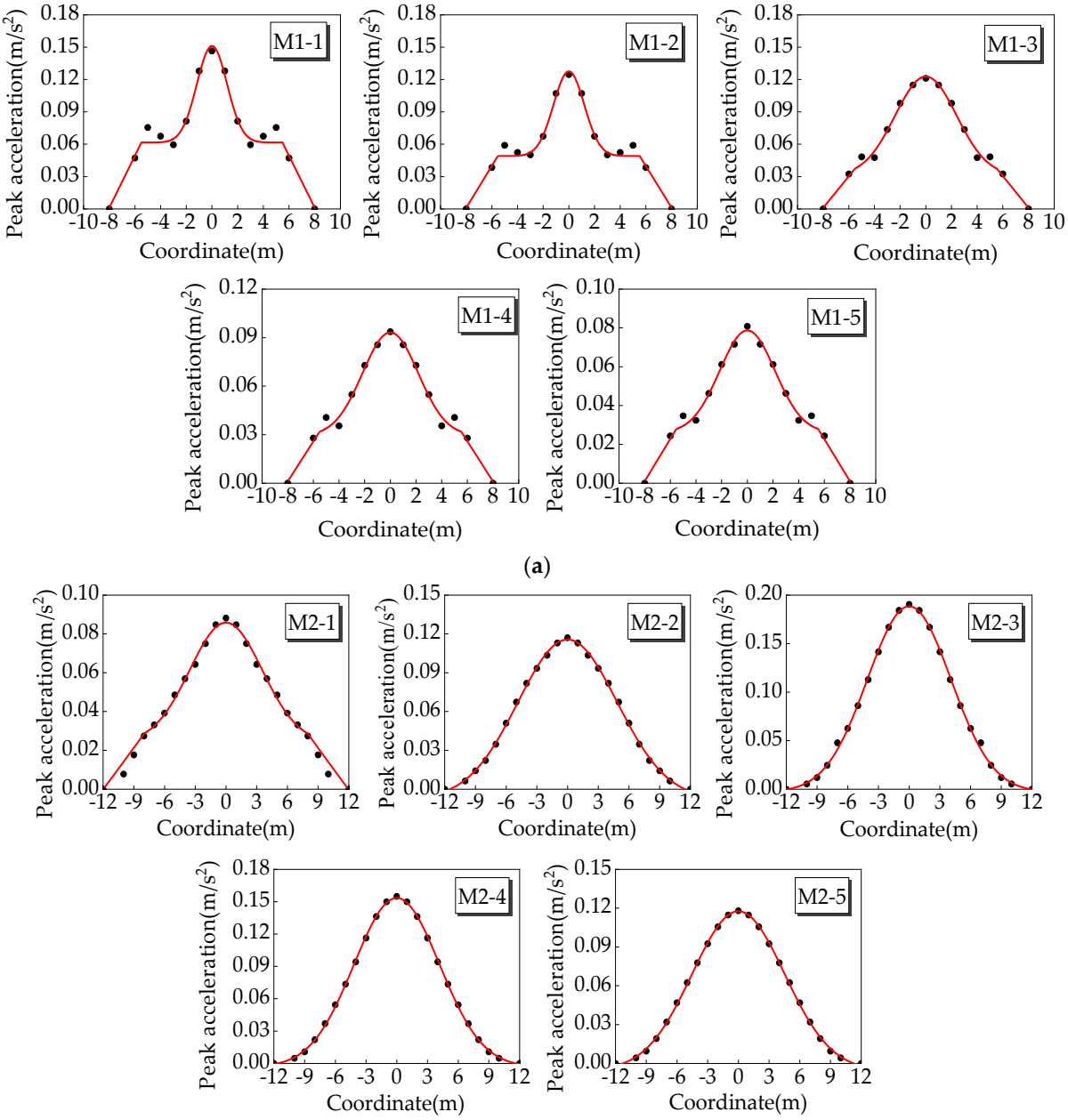

Figure 16. Nonlinear fitting curves: (**a**) model M1; (**b**) model M2.

3.2.2. Model Quality Assessment

Assuming that the numerical results were reliable, the accuracy of the regression model had to be evaluated [33]. In the regression analysis, the regression effect was characterized by the R^2 (coefficient of determination), and R was the ratio of the sum of regression square and the sum of total deviation square in the regression analysis. The larger the value, the more accurate the model was and the more significant the regression effect was. The R^2 can be calculated according to Equation (9):

$$R^2 = 1 - \frac{\sum(y - \hat{y})^2}{\sum(y - \overline{y})^2} \tag{9}$$

where $\hat{y}$ is the estimated value, $\overline{y}$ is the mean value, and y is the actual value.

In this paper, the estimated value $\hat{y}$, mean value $\overline{y}$, and actual value y corresponded to the calculated value of the finite element, the fitting value of the parametric model, and the mean value of the calculated value of the finite element model, respectively; the above parameters were brought into Equation (9). The calculated values are shown in Table 8. The natural frequencies of the models M1-1−M2-1 were 2.29−5.53 Hz, which were different from the human excitation frequency of 2 Hz, and since it was not easy to resonate, it was fitted according to the nonresonant model. The natural frequency of models M2-2−M2-5 was between 1.95 and 2.11 Hz, which was very close to the human induced excitation frequency of 2 Hz, and since it was very easy to resonate, it was fitted according to the resonant model.

Table 8. Parameter values of curve model.

Model		*c*	*A*	*w*	R^2	Adjusted R^2
M1	M1-1	0.186	0.089	1.18	0.92	0.89
	M1-2	0.147	0.079	1.2	0.95	0.93
	M1-3	0.093	0.092	2.39	0.98	0.97
	M1-4	0.087	0.064	2.17	0.97	0.96
	M1-5	0.078	0.053	2.15	0.98	0.97
M2	M2-1	0.072	0.062	3.54	0.99	0.99
	M2-2	-	0.123	4.85	0.99	0.99
	M2-3	-	0.19	4.08	0.99	0.99
	M2-4	-	0.157	4.18	0.99	0.99
	M2-5	-	0.123	4.52	0.99	0.99

It can be seen in Table 8 that the R^2 values for all models were between 0.89 and 0.99, indicating that the acceleration plane distribution model established in this paper had a very good fitting effect on the finite element calculation values.

3.3. Experimental Verification of Distribution Model

The New Museum of Guizhou Province is located in Guiyang City, Guizhou Province, China. The main structure was completed in September 2014, and various forms of long-span Vierendeel sandwich plates were adopted. In this paper, a steel–concrete composite Vierendeel sandwich plate with a 15.6 m × 17.5 m span orthogonal and upright grid was selected for analysis. Its location and a site photo are shown in Figure 17. The top (bottom) chords are T-shaped steel, the shear connectors are square steel pipe, one side of the floor is supported by the shear wall, and the other three sides are supported by the format frame wall.

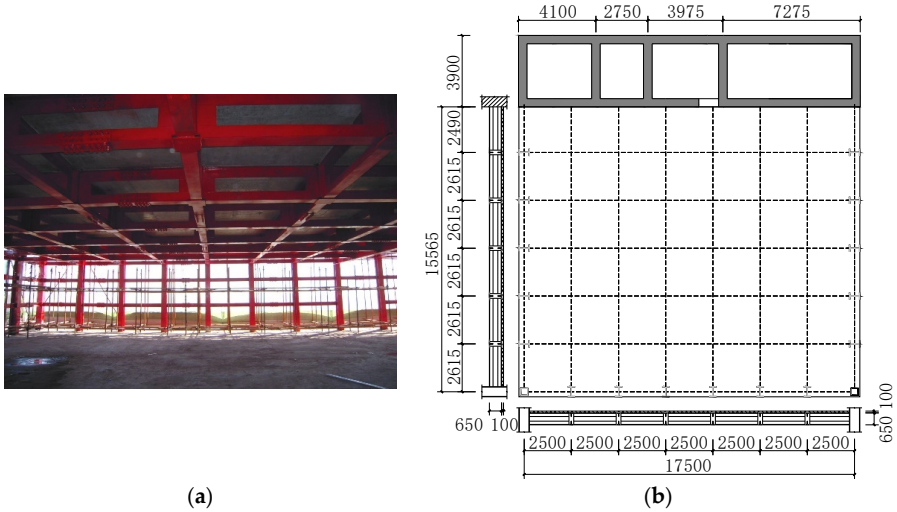

(**a**) (**b**)

Figure 17. Structural diagram of the floor: (**a**) site photo; (**b**) plane layout.

There are five floors of the long-span floor, which are used as a conference hall and 5D cinema, respectively. Cinemas and conference rooms are large public buildings with high crowd densities. Under crowd excitation, their comfort degree affects the experience and satisfaction of tourists during operation. Because the evaluation of the floor comfort degree is mostly related to the structural dynamic response, the acceleration response distribution amplitude is taken as the index, and through the analysis of human-induced-vibration response of the floor, the dynamic characteristics of the steel Vierendeel sandwich plate can be deeply understood.

A 15.6 m × 17.5 m span Vierendeel sandwich plate in the New Museum of Guizhou Province was tested on site. The geometric center of the floor was selected as the point of excitation, and the excitation method was a single person standing in place. The experimental equipment mainly included five TST126V dynamic signal sensors and a TAISITE TST5912 dynamic signal acquisition and analysis system. The test site and five acceleration sensors (A~E) were arranged as shown in Figure 18. In the experiment, the tester was instructed to march on the spot at a step frequency of 2.0 Hz for 30 s at the center of the sandwich plate. The acceleration sensors were used to collect the response signals at different positions; the data acquisition time was 1 min and the frame rate was 100 Hz. After the collection, the data were preliminarily sorted, and the acceleration responses of different measuring points on the floor during this period were analyzed; thus, the peak acceleration of the floor at different positions could be obtained.

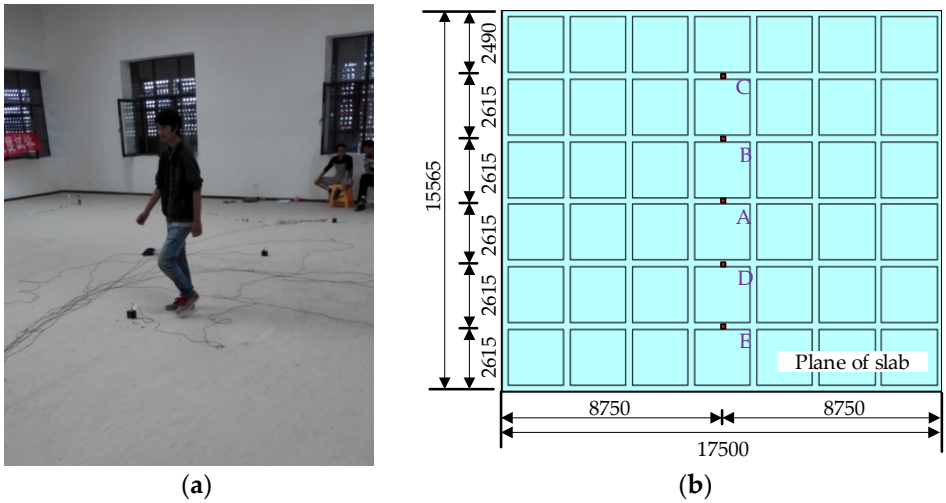

Figure 18. Dynamic response test: (**a**) test site; (**b**) layout position of acceleration sensors.

According to the actual measurement size, the finite element model of the 15.6 m × 17.5 m span open-web sandwich plate was established at a ratio of 1:1. The translational and rotational degrees of freedom of the grid intersections around the floor were constrained. We set the point of excitation at the geometric center of the floor (point A) for the transient analysis, and peak acceleration responses at different locations on the floor are recorded. The nonlinear curve was fitted to the finite element calculation results according to Equation (6) to obtain the model curve. A comparison between the model curve and the peak acceleration response of the measured points (A~E) on the project site is shown in Figure 19. It can be seen in Figure 19 that the model curve was consistent with the measured data. Table 9 shows a comparison between the fitting results and the measurement results for each measuring point. The maximum measurement error was less than 6%, indicating that the method proposed in this paper could effectively calculate the acceleration distribution characteristics of the sandwich plate.

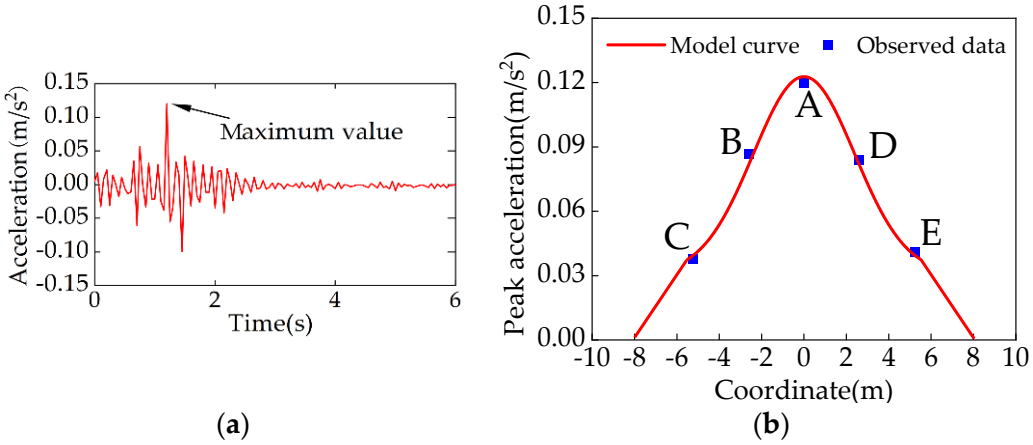

Figure 19. Peak acceleration response: (**a**) acceleration responses at position "A"; (**b**) measured acceleration value and model curve.

Table 9. Comparison of measurement results.

Sensor Location	Fitting Value (m/s^2)	Measured Value (m/s^2)	Error (%)
A	0.123	0.120	2.50%
B	0.082	0.087	5.74%
C	0.039	0.038	2.63%
D	0.082	0.084	2.30%
E	0.039	0.041	4.88%

4. Comfort Evaluation Method Based on Comfort Assurance Rate

At present, when evaluating the comfort degree, the peak response evaluation criterion is adopted in the codes of various countries; that is, the response of the floor under a human-induced load is not greater than the specified value. However, through the analysis conducted in this paper, it was found that for the large-span steel Vierendeel sandwich plate structure, the response peak distribution was funnel-shaped (Figure 7). The area with a large response only accounted for a small part of the total area of the floor. The maximum value was located in the center of the floor, and decayed sharply to the surrounding areas. In addition, the value at each point of the floor was also the maximum value on the acceleration response time history curve, and the duration of the maximum value accounted for a very small proportion of the entire response process, as shown in Figure 20. In addition, the maximum value on the acceleration response time history curve was taken as the value of each point of the floor, and the duration of the maximum value accounted for a very small proportion of the entire response process, as shown in Figure 20. Therefore, we found that the current peak acceleration evaluation scheme commonly used in engineering is too conservative. This paper attempted to establish a comfort evaluation method based on the floor area comfort assurance rate.

To reflect the proportion of the area with an acceleration response on the floor that was less than a certain value in the total floor area, we introduced coefficient λ, which we defined as the floor comfort assurance rate. According to the definition, it can be calculated according to Equation (10):

$$\lambda = 1 - \frac{\pi r^2}{L^2} \tag{10}$$

where r is the radius of the circular area when the peak acceleration response on the floor was greater than a and L is the side length (or span) of the floor, as shown in Figure 21.

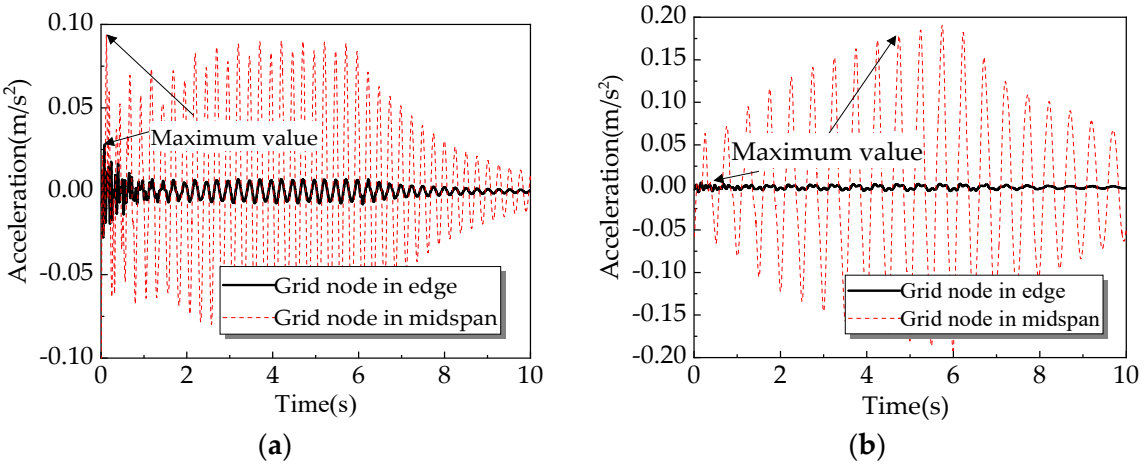

Figure 20. Response time history curves of two human-induced-vibration states: (**a**) resonance; (**b**) nonresonance.

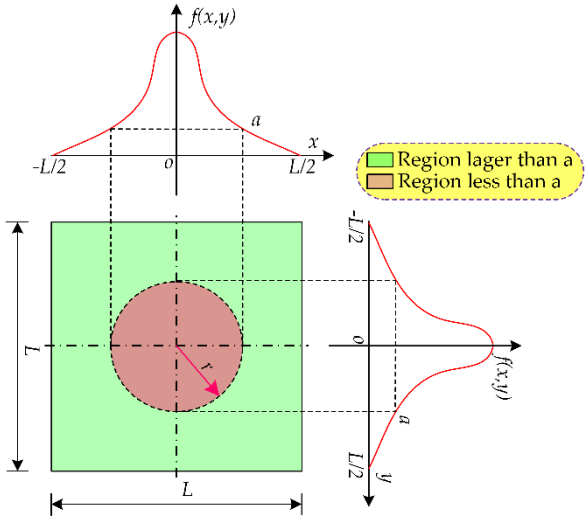

Figure 21. Schematic diagram of floor comfort assurance rate.

Referring to the unified standard reliability design of building structures (GB50068-2018) [34], we took the peak acceleration $a_{0.95}$ corresponding to λ = 95% as the representative value of the floor acceleration response and compared it with the specification limit (Equation (11)) used for comfort evaluation:

$$a_{0.95} \leq [a] \tag{11}$$

where a is the allowable value of the specification for human-induced-vibration acceleration; the value can be taken from Refs. [35,36].

We substituted λ = 95% into Equation (10) to obtain:

$$r = \sqrt{\frac{L^2}{20\pi}} \tag{12}$$

We substituted Equation (12) into Equations (5) and (6) to obtain the representative value of the acceleration response under resonance and nonresonance, which could be calculated according to Equations (13) and (14), respectively:

$$a_{0.95} = Ae^{-\frac{r^2}{2w^2}} = Ae^{-\frac{L^2}{40\pi w^2}} \tag{13}$$

$$a_{0.95} = \frac{c}{3} + Ae^{-\frac{x^2+y^2}{2w^2}} = \frac{c}{3} + Ae^{-\frac{L^2}{40\pi w^2}} \quad (14)$$

By substituting the fitting values of the parameters in Table 8 into Equations (13) and (14), the representative value of the acceleration response of the floor could be obtained. The comfort performance of the floor was evaluated using Equation (11).

For the numerical example in this study, the evaluation method used was compared with the maximum evaluation method; the relationship between the values of $a_{0.95}$ and a_{max} are shown in Table 10.

Table 10. Numerical size relationship between different models ($a_{0.95}$ and a_{max}).

Model		$a_{0.95}$ (m/s^2)	a_{max} (m/s^2)	$a_{0.95}/a_{max}$	Model		$a_{0.95}$ (m/s^2)	a_{max} (m/s^2)	$a_{0.95}/a_{max}$
M1	M1-1	0.0826	0.1465	56.39%	M2	M2-1	0.067	0.0882	75.99%
	M1-2	0.0682	0.1246	54.73%		M2-2	0.1012	0.117	86.51%
	M1-3	0.0954	0.1211	78.78%		M2-3	0.1443	0.1904	75.77%
	M1-4	0.0705	0.0936	75.32%		M2-4	0.1208	0.1549	77.97%
	M1-5	0.0601	0.0809	74.35%		M2-5	0.0983	0.118	83.29%

It can be seen in Table 10 that the percentage of $a_{0.95}$ in a_{max} was affected by the span, concrete slab thickness, and whether resonance occurred. Overall, it was between 54.73% and 86.51%. In the case of nonresonance, the proportion of $a_{0.95}$ in a_{max} was between 54.73% and 78.78%. In the case of resonance, the proportion of $a_{0.95}$ in a_{max} was between 75.77% and 86.51%. It can be seen in the above analysis that the representative value of the evaluation could be greatly reduced by using $a_{0.95}$ to avoid being too conservative.

5. Conclusions

(1) Human-induced acceleration was affected by the span of the sandwich plate and the thickness of the concrete plate. The calculation results were affected by the grid size to a certain extent, and were less affected by the chord height and shear connector thickness;
(2) An acceleration response distribution model was established to accurately evaluate the dynamic response of a steel Vierendeel sandwich plate under human-induced fixed-point excitation;
(3) In view of the conservative peak acceleration evaluation scheme in engineering, this paper proposed a comfort evaluation method based on the floor area guarantee rate.

Author Contributions: Conceptualization, L.J. and R.C.; methodology, L.J.; software, H.Z.; validation, K.M.; formal analysis, R.C.; investigation, L.J.; resources, K.M.; data curation, L.J.; writing—original draft preparation, R.C.; writing—review and editing, L.J.; visualization, H.Z.; supervision, L.J.; project administration, K.M.; funding acquisition, L.J. All authors have read and agreed to the published version of the manuscript.

Funding: This research was funded by the Open Foundation Project of the State Key Laboratory for Safety Control and Simulation of Power System and Large Power Generation Equipment under grant number SKLD21KM11, as well as Key research and development projects in Hubei Province under grant number 2020BAB110.

Informed Consent Statement: Informed consent was obtained from all subjects involved in the study.

Data Availability Statement: Data will be shared upon request and consideration of the authors.

Conflicts of Interest: The authors declare no conflict of interest.

References

1. Wang, C.; Chang, W.S.; Yan, W.; Huang, H. Predicting the human-induced vibration of cross laminated timber floor under multi-person loadings. *Structures* **2021**, *29*, 65–78. [CrossRef]
2. Xie, Z.; Hu, X.; Du, H.; Zhang, X. Vibration behavior of timber-concrete composite floors under human-induced excitation. *J. Build. Eng.* **2020**, *32*, 101744. [CrossRef]
3. Cao, L.; Liu, J.; Li, J.; Zhang, R. Experimental and analytical studies on the vibration serviceability of long-span prestressed concrete floor. *Earthq. Eng. Eng. Vib.* **2018**, *17*, 417–428. [CrossRef]
4. Xiong, J.; Chen, J.; Caprani, C. Spectral analysis of human-structure interaction during crowd jumping. *Appl. Math. Model.* **2020**, *89*, 610–626. [CrossRef]
5. Jiang, L.; Ma, K.; Zhang, H.; Wu, Q.; Yang, Q. Seismic behavior of shear connectors of steel vierendeel sandwich plate. *Math. Probl. Eng.* **2019**, *2019*, 8047393. [CrossRef]
6. Harper, F.C. The mechanics of walking. *Res. Appl. Industry* **1962**, *15*, 23–28.
7. Kerr, S.C.; Bishop, N. Human induced loading on flexible staircases. *Eng. Struct.* **2001**, *23*, 37–45. [CrossRef]
8. Chen, J.; Wang, H.; Peng, Y. Experimental investigation on Fourier-series model of walking load and its coefficients. *J. Vib. Shock* **2014**, *33*, 11–15+28.
9. Ding, G.; Chen, J. Influences of walking load randomness on vibration responses of long-span floors. *J. Vib. Eng.* **2016**, *29*, 123–131.
10. *AISC811-97*; Steel Design Guide 11: Floor Vibrations due to Human Activity. American Institute of Steel Construction: Chicago, IL, USA, 1997.
11. Hakim, L. *PCI Design Handbook*, 7th ed.; Precast/Prestressed Concrete Institute: Chicago, IL, USA, 2010.
12. *Concrete Society Technical Report 43: Appendix G*, 2nd ed.; The Concrete Society: Surrey, UK, 2005.
13. *CCIP-016*; Standard for a Design Guide for Footfall Induced Vibration of Structures. The Concrete Centre: London, UK, 2007.
14. Parkhouse, J.G.; Ewins, D.J. Crowd-induced rhythmic loading. *Proc. Inst. Civil. Eng. Struct. Build.* **2006**, *159*, 247–259. [CrossRef]
15. Chen, J.; Peng, Y.; Wang, L. Experimental investigation and mathematical modeling of single footfall load using motion capture technology. *Chin. J. Eng. Des.* **2014**, *47*, 79–87. [CrossRef]
16. Zivanovic, S.; Pavic, A.; Reynolds, P. Vibration serviceability of footbridges under human-induced excitation: A literature review. *J. Sound Vibr.* **2005**, *279*, 1–74. [CrossRef]
17. Zhu, Q.; Liu, L.; Du, Y.; Chen, K. Human-induced vibration and control for cantilever steel bar truss deck slab based on pedestrain-structure interaction. *J. Build. Struct.* **2018**, *39*, 99–108.
18. Cao, L.; Li, A.; Zhang, Z.; Zhou, D.; Zhou, C. Human-induced vibration analysis and measurement of long-span composite floors. *J. Southwest Jiaotong Univ.* **2012**, *47*, 922–928.
19. Wang, Z.; Li, X.; Yi, J.; Li, Q. Human-induced vibration and optimal control of long-span glulam arch bridges. *China Civil. Eng. J.* **2021**, *54*, 79–94.
20. Jiang, L.; Ma, K.; Zhang, H.; Yang, Q.; Huang, J. Dynamic time-history analysis of large span open-web sandwich plate for vibration comfort based on walking route method. *Spat. Struct.* **2016**, *22*, 28–36+43.
21. *BS 5400*; Steel, Concrete and Composite Bridges-Part 2: Specification for Loads. British Standards Institution: London, UK, 2006.
22. Gulvanessian, H.; Calgaro, J.A.; Holický, M. *Designers' Guide to EN 1990 Eurocode: Basis of Structural Design*; Thomes Telford: London, UK, 2002; pp. 52–69.
23. *ISO10137*; Bases for Design of Structures-Serviceability of Buildings and Walkways against Vibrations. International Organization for Standard: Genève, Switzerland, 2007.
24. HiVoSS. *Human Induced Vibrations of Steel Structures: Design of Footbridges*; RFS2-CT-2007-00033, Footbridge_Guidelines_EN03; European Communities: Luxembourg, 2008.
25. *GB50010-2010*; Code for Design of Concrete Structures. China Construction Industry Press: Beijing, China, 2010.
26. *JGJ3-2010*; Technical Specification for Concrete Structures of Tall Building. China Construction Industry Press: Beijing, China, 2010.
27. Fiore, A.; Marano, G.C. Serviceability performance analysis of concrete box girder bridges under traffic-induced vibrations by structural health monitoring: A case study. *Int. J. Civ. Eng.* **2017**, *16*, 553–565. [CrossRef]
28. Jiang, L.; Ma, K.; Zhang, H.; Xu, X.; Wei, Y.; Hu, L. The dynamic property and comfort degree study on the steel-concrete composite vierendeel sandwich plate. *Earthq. Eng. Struct. Dyn.* **2017**, *6*, 122–131.
29. Blanchard, J.; Davies, B.L.; Smith, J.W. Design criteria and analysis for dynamic loading of footbridges. In Proceedings of the Symposium on Dynamic Behaviour of Bridges, Crowthorne, UK, 19 May 1977.
30. Matsumoto, Y.; Nishioka, T.; Shiojiri, H. *Dynamic Design of Footbridges*; Heft P-17; International Association for Bridge and Structural Engineering: Zürich, Switzerland, 1978.
31. Han, X.; Chen, X.; Mao, G.; Zheng, Y.; Ji, J. Research on analysis method for floor vibration and formula derivation of response spectra based on simulation of crowd walking. *Build. Sci.* **2009**, *5*, 4–9.
32. Lou, Y.; Huang, J.; Lv, Z. *Vibration Comfort Evaluation of Floor System*; Science Press: Beijing, China, 2012.
33. Xue, J.; Fiore, A.; Liu, Z.; Briseghella, B.; Marano, G.C. Prediction of ultimate load capacities of CFST columns with debonding by EPR. *Thin-Walled Struct.* **2021**, *164*, 107912. [CrossRef]

34. *GB50068-2018*; Unified Standard for Reliability Design of Building Structures. China Architecture & Building Press: Beijing, China, 2018.
35. *JGJ99-2015*; Technical Specification for Steel Structure of Tall Building. Ministry of Housing and Urban-Rural Development of the People's Republic of China. China Architecture & Building Press: Beijing, China, 2016.
36. *JGJ/T441-2019*; Technical Standard for Human Comfort of the Floor Vibration. China Architecture & Building Press: Beijing, China, 2019.